Environmental Resources Research
Vol. 8, No. 1, 2020

GUASNR

Applications of goethite nanoparticles for removal of arsenic and mercury toxic ions from synthetic wastewater

M. Mojarad Farimani[1], R. Dabiri[2*]
[1]PhD candidate, Department of Geology, Mashhad Branch, Islamic Azad University, Mashhad, Iran
[2]Associate professor, Department of Geology, Mashhad Branch, Islamic Azad University, Mashhad, Iran

Received: March 2019 ; Accepted: June 2020

Abstract

Contamination of water resources with toxic elements is one of the challenges of the today's world. In this research, application of Goethite nanoparticles in removing contamination of arsenic and mercury from synthetic wastewater in a batch mode is investigated. For this purpose, the effect of different factors including pH, adsorbent dosage, contact time, and initial concentration on the extent of adsorption of arsenic and mercury by the Goethite nanoparticles was studied. The maximum extent of arsenic adsorption in this study being 99.95% occurred at pH=4, adsorbent dose of 4 g/L, initial concentration of 10 mg/L and after 120 min from the beginning of the reaction. Examination of the effect of pH on the extent of mercury adsorption showed that the maximum mercury adsorption occured at pH=8. Furthermore, the adsorbent dose of 3 g/L with initial concentration of 10 mg/L, following 30 min from the beginning of the reaction caused mercury removal from aqueous solution by up to 72.45%. Investigation of the equation of isotherms of Langmuir and Freundlich adsorption for arsenic and mercury shows better congruence of these ions with Langmuir isotherms. The kinetic studies showed that the As and Hg adsorption mechanism was well described by pseudo-second-order kinetic model. This study indicates that Goethite nanoparticles could be used for removing the toxic arsenic and mercury ions from wastewater.

Keywords: Goethite nanoparticles, Arsenic, Mercury, Water Pollution, Adsorption.

[*]Corresponding author; rahimdabiri@yahoo.com

Introduction

Water quality is one of the main challenges that societies are facing during the 21st century, threatening human health, limiting food production, reducing ecosystem functions, and hindering economic growth. The availability of the world's scarce water resources is increasingly limited due to the worsening pollution of freshwater resources caused by the disposal of large quantities of insufficiently treated, or untreated, wastewater into rivers, lakes, aquifers and coastal waters. One of the important sources of water contamination is entrance of toxic elements into water resources (Milačič et al., 2019). There are over 50 elements that can be classified as heavy metals (Bolong et al., 2009). Arsenic, mercury, lead, and cadmium are the most common metals that play important role in human toxicity. Heavy metals such as copper, zinc, and chromium are required for human body at trace amounts, but these elements can cause toxicity at large amounts. In order to overcome this problem and also to solve the environmental problems caused by their presence, one option is to remove them from the source of wastewater. Among removal methods, adsorption technique has attracted the attention of many researchers due to being easy, cost-effective, highly efficient and regenerative. Meanwhile, application of iron nanoparticles is more common owing to high reactivity, high adsorption potential, and more effective clearance (Grieger et al., 2010). Experimental studies have also shown that iron nanoparticles are able to degrade very stable contaminations (including perchlorate, halogen-containing hydrocarbons, nitrate, and the ions of heavy metals) (O'Carroll et al., 2013). The chemical composition of iron oxides has indicated that these compounds are composed of layers containing bi- and trivalent iron in the vicinity of a metal kernel. Following exposure to water space, the oxidized surface equally contains hydroxide groups, thereby developing a certain level of FeOOH (Yang et al., 2010). Goethite is an iron oxide that is used in many pieces of research thanks to its surface chemistry, chemical structure, morphology, and frequency (Jacobson and Fan, 2019; Su et al., 2019; Vollprecht et al., 2019). The main goal of this study was to remove arsenic and mercury toxic ions from synthetic wastewater by using goethite nanoparticles adsorbent and to investigate the influence of different parameters involved during the sorption process such as contact time, metal ion concentration and pH. This adsorbent was characterized using Scanning Electron Microscope (SEM), Fourier Transform Infrared spectroscopy (FTIR), X-ray Diffraction (XRD), Dynamic Light Microscope (DLS) and pHzpc (point of zero charge). Also, the kinetic and equilibrium parameters and adsorption isotherm models were investigated.

Materials and Methods

Preproduction of the adsorbents

In this study, all the chemicals were provided with high-percentage purity from the Merck Group (Germany). Synthetic goethite, FeOOH, is often used as a model system in laboratory studies of adsorption (Blesa et al., 1997; Kosmulski, 2001). The Goethite nanoparticles used in this work were synthesized by 100 ml $Fe(NO_3)_3$ 1M solution. This solution was poured into a 2-L polyethylene container, to which 180 ml KOH solution was added when being stirred. Furthermore, during the stirring process, the volume of the solution was quickly brought to 2 L by deionized water. The obtained solution was then placed inside an oven at 70 °C for 60 h (Schwertmann and Cornell 2008). Thereafter, the solution was passed through a syringe filter (0.22 µm) and then washed with distilled water four times and finally the residual solution was dried at room temperature. In this method, 9 g Goethite was obtained at a nano size. In order to improve the repeatability of the results, all the experiments repeated three times and the mean of the three measurements was reported. Fourier transform infrared (FT-IR) spectra were obtained under dry air at room temperature on KBr pellets in the range 4000-500 cm^{-1}. The pH_{PZC} at which the adsorbent is neutral in aqueous suspension, was determined following the

procedure of Lopez-Ramon et al. (1999). In this method, 50 ml of 0.01M NaCl solutions was poured in closed Erlenmeyer flasks under agitation at room temperature of about 25 °C. The pH of each solution was initially fixed at value lying from 2 to 12 by adding 0.1M HCl or 0.1M NaOH solutions. Then 0.1g of solid adsorbent was added to each flask and the final pH was measured after 48 h. pH_{PZC} is localized at the point where the curve pH_{final} versus $pH_{initial}$ intersects the first bisector. Statistical analysis, calculation of the data and linear least square fitting was carried out using SPSS software.

The characteristics of the adsorbent

X-Ray diffraction (Xrd)

In order to examine the compositions and crystal structure of the samples, XRD device of the mineralogy laboratory of Zarazma Minerals Company was used. The sample was analyzed by Philips-PW1800 at an angle of 5-60 2θ degrees by a copper tube under the voltage 40 kw and current's intensity 30 mA a using monochromatic ray of CuKa (λ=1.54 Å) As can be observed in Figure 1, the particles are only composed of Goethite particles and its sharp peaks represent the crystallization of these particles.

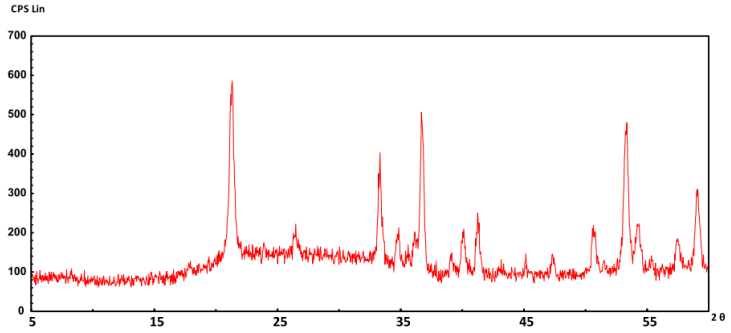

Figure 1. XRD pattern of Goethite nanoparticles sample.

Dynamic light microscope (dls) analysis of the particles

In order to investigate the dimensions and size distribution of the Goethite grains, dynamic light scattering (DLS) analysis was performed in Research Center of Mashhad by SZ-100 Nanoparticle Analyzer (Horiba). As the results of the analysis showed, the mean diameter of its particles was 45.22 nm, and its $Z_{average}$ was 148.93 nm (Figure 2). The diagram of the distribution of particles' size indicates over 99% of the particles have a size below 100 nm. Furthermore, the particles with the size of 22-46 nm have the greatest frequency.

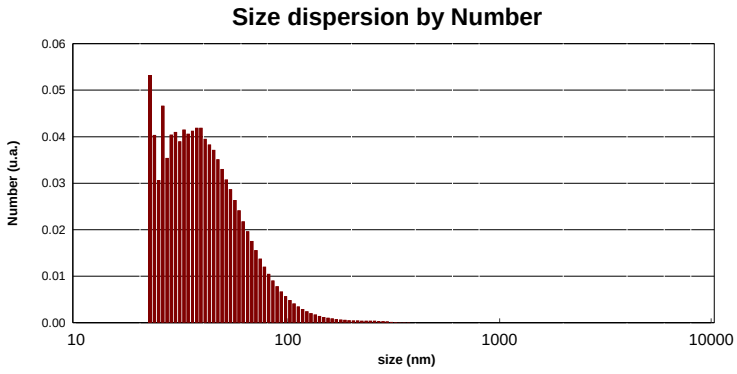

Figure 2. Particle size distribution of goethite synthesized nanoparticles.

Scanning electron microscopy (SEM)

To analyze the morphology, particle size, and shape of the Goethite nanoparticles, Scanning electron microscope (SEM) device of Razi metallurgy research Center was employed. The Backscatter images obtained from the SEM device with VEGA\\TESCAN-XMU model reveal that the majority of the particles have a size between 35 and 45 nm. These results are in congruence with the DLS results. As can be observed in Figure 3, the distribution of the particles is suitable and uniform and the shape of the majority of the particles is needle-like.

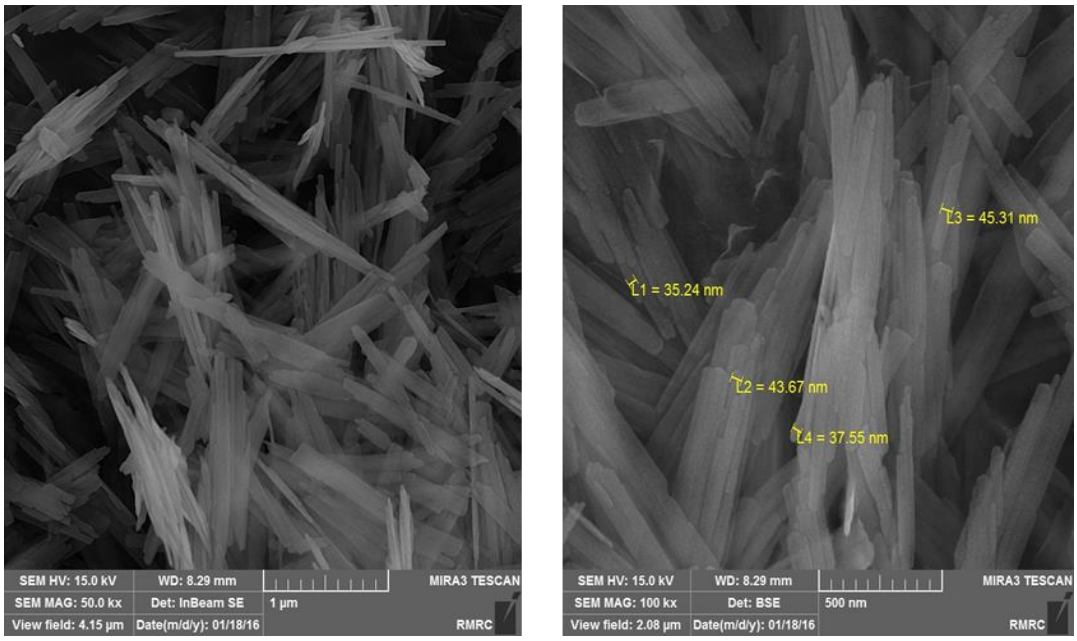

Figure 3. Structure, morphology, particle size, and shape of goethite nanoparticles.

Ir spectroscopy

In order to confirm the presence of the toxic ions (As and Hg) on the sorbents, FT-IR analyses were conducted before and after the adsorption process and chemical modification (Figure 4). FTIR spectrums were recorded with a Nicolet, Avatar 370 spectrometer at the Ferdowsi University of Mashhad, Iran. The bands centered at Σ630-640 cm^{-1} can be all identified to be the Fe–O vibrational modes in FeOOH, the bands at 790-800 cm^{-1} and 890-900 cm^{-1} are characteristic of FeOOH, and thus they can be assigned to Fe–O–OH bending vibrations modes in FeOOH (Cambier, 1986; Chen et al., 2011; Cwiertny et al., 2008; Musić et al., 2004). The band centered at Σ1650 cm^{-1} can be identified to be O–H stretching mode in the goethite structure. The FTIR spectra revealed a strong and broad band between 3000 and 3600 cm^{-1}, which was associated with the O-H stretching vibrations of the hydroxyl groups in the layers and interlayer water molecules (Liu et al., 2008). Comparison of fresh and contaminated goethite samples shows no major differences, signifying the stability of the goethite sample after adsorption. In the after absorption spectrums, Fe-O-H vibrations shift to higher frequencies and Fe-O-Hg/As vibrations. Peaks related to arsenic and mercury adsorption are not very distinct due to their low concentrations.

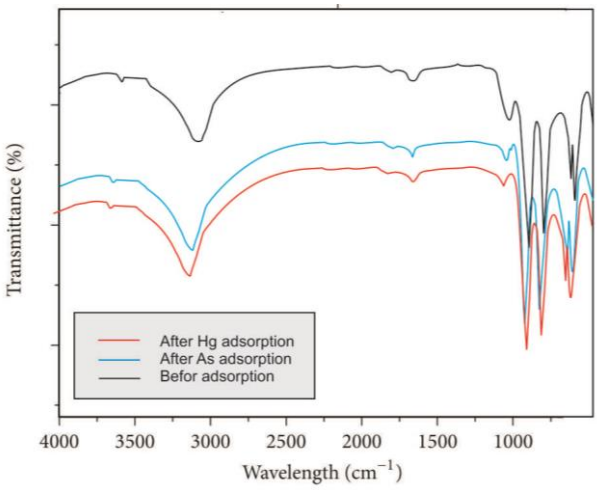

Figure 4. FT-IR spectra for nanogoethite before and after As and Hg adsorption.

Adsorption experiments

Batch adsorption experiments were conducted for removal of arsenic and mercury from wastewater by goethite nanoparticles adsorbent. The arsenic and mercury solution used in these experiments was prepared by dissolving the white powder of sodium arsenate ($Na_2HAsO_4.7H_2O$) and the white powder of mercury chloride (II) in distilled water. First, a concentrated solution was prepared with a concentration of 500 ppm and then the required solutions were prepared with different concentrations through diluting it. For each stage of the experiment, a standard solution (control) was also prepared, that was sent to Mashhad Ferdowsi laboratory together with other samples for ICP-OES analysis, with the extent of arsenic and mercury adsorption being measured against it.

Results and Discussion

The effect of solution pH on the adsorption of arsenic and mercury

In order to examine the effect of the solution's pH on the mechanism and the capacity of adsorption process of arsenic and mercury, adsorption tests were performed at pHs=2, 4, 6 and 8, initial concentration of 10 mg/L for the ions, adsorbent's dose of 2, and time of 60 min under laboratory temperature conditions. As can be seen in Figure 5, the maximum adsorption for arsenic has occurred at pH=4, while for mercury, it has taken place at pH=8. At a pH below 4, pentavalent arsenic is in the form of H_3AsO_3, which has a neutral charge. At pH=4, the only form of arsenic present in the solution is $H_2AsO_4^-$. Furthermore, at pH above 4, there is no neutral particle in the solution and the oxyanions present in the solution have a negative charge (Wang et al., 2000). With the increase in pH, the extent of $H_2AsO_4^-$ diminishes, while $HAsO_4^{2-}$ level grows. In other words, as the environment becomes alkaline, the extent of positive charge diminishes gradually, thereby causing decreased extent of adsorption of arsenate ions (Tripathy and Raichur, 2008). Results showed that the maximum extent of adsorption occurs in pH=4 by 92.71%. Furthermore, the maximum extent of adsorption capacity in these conditions will be 4.63. Considering mercury, at low pH (acidic environment), the concentration of H^+ ion in the solution is high and the more we approach lower pH, the higher this value becomes. With the increase in pH, the concentration of protons declines and therefore the competition is dropped, and thus a greater mercury ion is adsorbed by the adsorbent. At low pH, protons occupy the surface of the adsorbent, and as its electrical charge is positive, it results in electrostatic repulsion, thereby preventing adsorption of mercury cations on the surface of the adsorbent. The concentration of OH^- ions increases, at high pH value. Consequently, it has no negative impact on the adsorption process (Lohani et al., 2008;

Sari and Tuzen, 2009). The maximum extent of adsorption is observed at pH=8 to be 78.12%, and the maximum adsorption capacity at pH=8 was 3.90. The adsorbent used in this work has an experimental pH PZC of 8.2. Therefore, at a pH value above pH PZC, the net charge on the adsorbent becomes negative, while at a pH value below pH PZC, the net surface charge becomes positive. Based on this, the negative charge increases with increase in the solution pH.

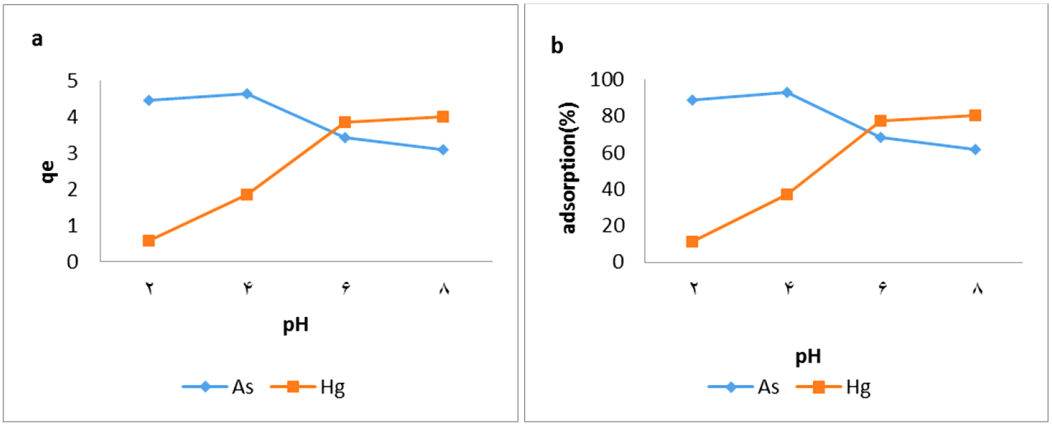

Figure 5. a) Influence diagram of pH on adsorption capacity of goethite nanoparticles. b) Influence diagram of pH on removal of arsenic and mercury by goethite nanoparticles.

The effect of adsorbent dose on the adsorption of arsenic and mercury

Adsorbent dose is a very important parameter in adsorption which determines the amount of removal as well as the economics of the process. Experimental results in Figure 6 showed that the adsorption capacity was increased with increase in adsorbent dosage. The maximum removal percentage for arsenic and mercury were seen at adsorbent's dose of 4 and 3 with respective values of 99.8 and 66.26%. The adsorbent's dose represents the number of available sites of the adsorbent for adsorption of toxic elements. Typically, the adsorption capacity diminishes with the increase in the adsorbent dose. This reduction is due to the sites which remain unsaturated along the adsorption process. Furthermore, with the increase in the adsorbent's dose, the accessibility of toxic elements ions to the remaining sites declines (Rashidi *et al.* 2010). The reason for the reduction of mercury removal beyond the adsorbent's dose of 3 is that goethite nanoparticles have become saturated by mercury ion, after which desorption takes place.

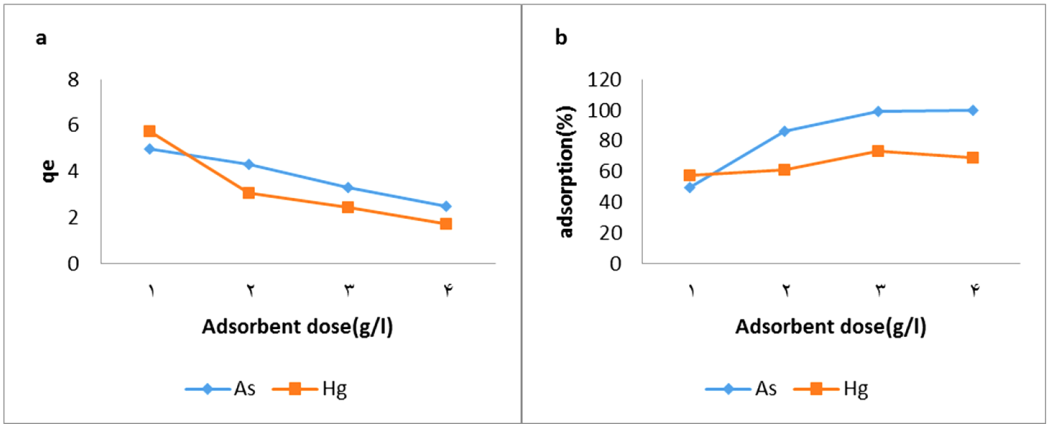

Figure 6. a) influence diagram of adsorbent dose on adsorption capacity of goethite nanoparticles. b) influence diagram of adsorbent dose of goethite nanoparticles on removal of arsenic and mercury.

The effect of contact time on adsorption of arsenic and mercury

The experimental effect of contact time on the extent of removal of arsenic and mercury ion in the solution was depicted in Figure 7. As can be seen, with increase in the contact time between arsenate ions with the active sites of the adsorbent, the adsorption capacity has also grown. The maximum removal percentage 99.87% was obtained at time of 2 h, with the maximum adsorption capacity being 2.496 during this time.

Considering mercury, the maximum adsorption level of 69.14% took place within 30 min, with the maximum adsorption capacity being 2.306. The adsorption active sites present on the adsorbent of goethite nanoparticles have been empty, at the beginning of the reaction. Once they get into contact with mercury ions, they adsorb them. These results show that over time the number of adsorption sites becomes vacant, thereby decreasing the adsorption rate. In addition, at the beginning of the reaction, the concentration slope which is the driving force of adsorption process has been very large and over time decreases. This reduction in the concentration slope has led to diminished adsorption rate. It is obvious that the extent of adsorption rises after 180 min, as a two-branched dual core complex establishes a bond with surface hydroxyls in bioctaeder genera of the adjacent $Fe(OH)_6$. Such a position is called a two-corner bond and is predominant on the goethite planes (101) (Cornell and Schwertmann, 2003). On the other hand, two branched singular core complexes, are in bond with the parallel groups of the edge of mono octahedral complex of $Fe(OH)_6$, and is called edge bond. The positions of these edges seem to be sites with a high energy which have preferably been occupied across surfaces with less coverage (Cornell and Schwertmann, 2003).

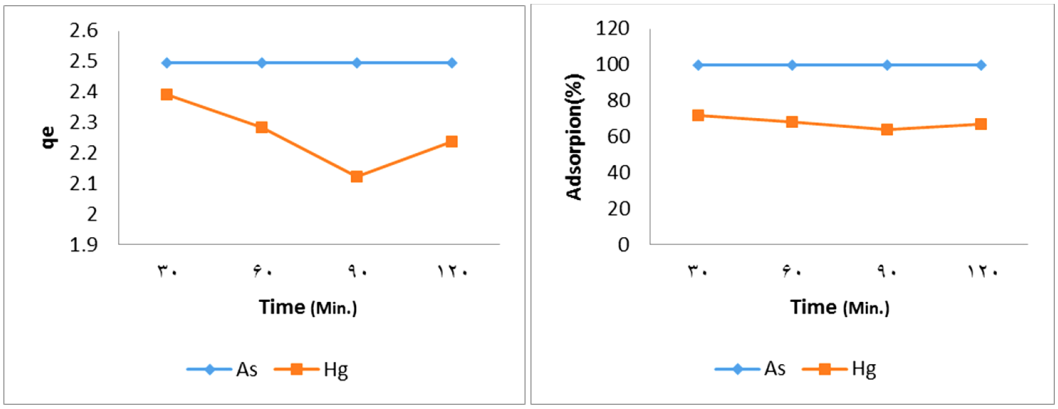

Figure 7. a) Influence diagram of contact time on adsorption capacity of goethite nanoparticles, b) Influence diagram of contact time on removal of arsenic and mercury by goethite nanoparticles.

The effect of the initial concentration on the adsorption of arsenic and mercury

Figure 8 demonstrates the effect of the concentration of arsenic and mercury ion on the adsorption of these ions from aqueous solution. The extent of adsorption capacity increases with increasing initial concentration. As shown in Figure 8, the maximum extent of adsorption has occurred at the 10 ppm concentration which is equal to 99.86%, with the maximum capacity of adsorption being 6.072 at the concentration of 50 ppm. Despite the constancy of the number of active sites, as the initial concentration increases, so does the concentration slope, thereby causing more ions to be adsorbed (Beck et al., 1992). Following the concentration of 10 ppm, the extent of adsorption declines.

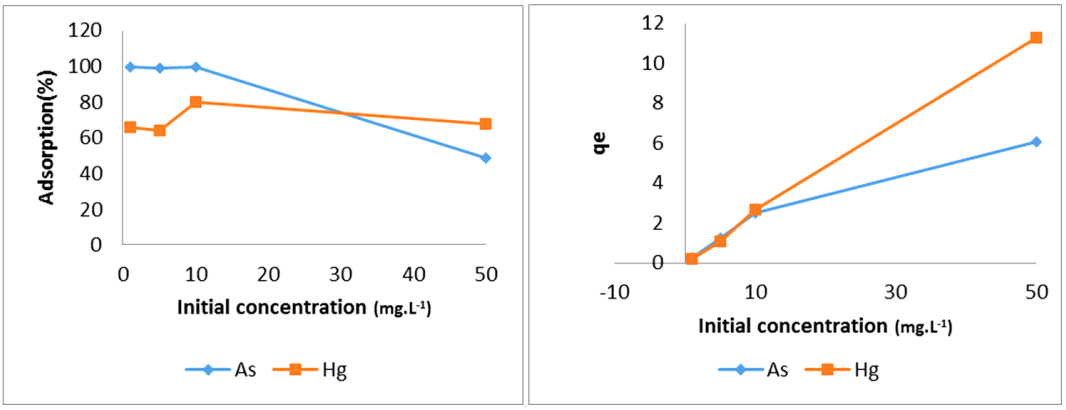

Figure 8. A) Influence diagram of initial concentration on adsorption capacity of goethite nanoparticles, b) Influence diagram of initial concentration on adsorption capacity of goethite nanoparticles.

Adsorption isotherms

Adsorption isotherms refer to a series of adsorption measurements performed at a given temperature and whose results are plotted as a relationship between adsorbed and non-adsorbed amounts. Adsorption isotherms are useful tools for understanding the mechanism of adsorption, adsorbate and adsorbent. It is possible to determine the free surface area of the adsorbent, the volume and distribution of the size of pores, the heat of adsorption process, and relative adsorption of gas or vapor on the adsorbent by using isotherm adsorption models. Several isotherm equations have been reported, yet the most important adsorption isotherms are Langmuir and Freundlich equations. In both chemical and physical adsorption, these two equations are of great significance (Bansal and Goyal, 2005).

Freundlich isotherms

Freundlich isotherm is one of the important models for isothermal adsorption surfaces. This model indeed represents evaluation of the difference between the liquid phase and the adsorbent. Freundlich offered this model on the fact that the adsorption sites and a solid body are nonuniform and their adsorption power is also different. He expressed his model through below equation:

$q_e=KC_e^{1/n}$

The logarithmic form of this equation is as follows:

$\log q_e=\log K + 1/n \log C_e$

In this equation, q_e and C_e are concentration of elements at equilibrium, n and k represent the Freundlich constants. If the curve is linear, adsorption process follows Freundlich model (Saxena et al., 2001).

Langmuir isotherms

This model was presented by Irvin Langmuir in 1916 (Langmuir, 1918). Langmuir isotherm accounts for the surface coverage by balancing the relative rates of adsorption and desorption (dynamic equilibrium). This equation is of great importance in both physical and chemical adsorption. This equation can be obtained by both static and thermodynamic methods (Bansal et al., 1971). This American scientist obtained equation based on some hypotheses, the most important of which are:

- The adsorbate components (molecules, atoms, or ions) are adsorbed on different sites of the solid surface.
- Each site adsorbs only one component.
- The adsorbent's surface is absolutely homogeneous and uniform and adsorption takes place in a monolayer fashion
- The adsorbate components reacts only with adsorption sites and have no interaction with each other (Bansal et al., 1970).

Langmuir equation is as follows:

$$\frac{1}{q_e}=\frac{1}{b}+\frac{1}{ab}*\frac{1}{C_e}$$

where, q_e is the amount of the solute adsorbed component per mass unit of the adsorbent in terms of mg/g, and C_e represents the remaining concentration in the solution in terms of mg/L, with a and b being the Langmuir constants. If the curve obtained from the points is linear, the adsorption mechanism is based on Langmuir model, otherwise it does not follow it (Saxena et al., 2001).

The arsenic adsorption isotherm by goethite nanoparticles

The Langmuir and Freundlich adsorption isotherms were used to describe the variable parameters of initial concentration. In Langmuir isotherm, the changes in q_e/C_e in relation with C_e, and in Freundlich isotherm the changes in $\log q_e$ in relation with variations of $\log c_e$ have been calculated. If the curves are linear, it represents that the adsorption process follows that model. As Figure 9 shows adsorption of arsenic by goethite nanoparticles, the Langmuir isotherm is monolayer and homogeneous. The correlation coefficient of R^2 in Langmuir and Freundlich models were 0.919 and 0.644, respectively. Table 1 presents the parameters of the calculated adsorption isotherms.

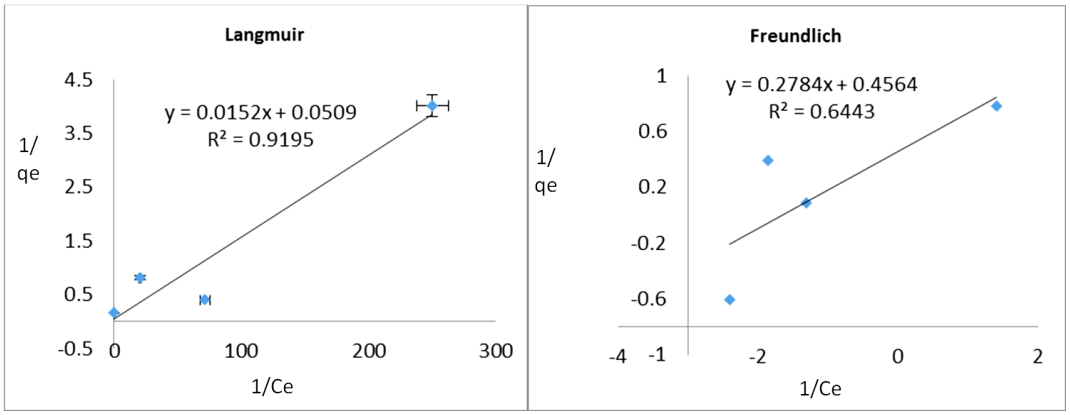

Figure 9. Langmuir and Freundlich isotherm on arsenic adsorption by goethite nanoparticles.

Table 1. Arsenic adsorption isotherm parameters by goethite nanoparticles.

Isotherm equations	Langmuir			Freundlich		
Coefficients	$q_{m\ (mg/g)}$	$B_{\ (L/mg)}$	R^2	$K_{f\ (mg/g)}$	n	R^2
Arsenic	19.64	3.414	0.9195	1.160	1.137	0.6443

Mercury adsorption isotherm by goethite nanoparticles

Figure 10 illustrates the Langmuir and Freundlich isotherm in terms of experimental data. These data have been investigated based on these two models linearly. As can be seen in the diagrams, adsorption of mercury by the goethite nanoparticles follows Langmuir model. This adsorption is monolayer and homogeneous in Langmuir model and the correlation coefficient R^2 in Langmuir model is 0.99, that clearly proves this matter. Freundlich isotherm with R^2 value 0.950 indicates multilayer adsorption. In Table 2, the parameters of the adsorption isotherms have been calculated.

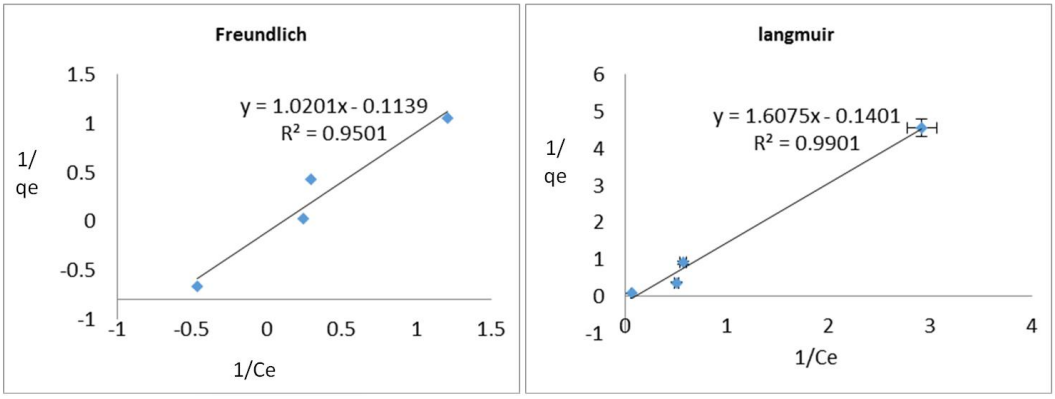

Figure 10. Langmuir and Freundlich isotherm on mercury adsorption by goethite nanoparticles.

Table 2. Mercury adsorption isotherm parameters by goethite nanoparticles.

Isotherm equations	Langmuir			Freundlich		
Coefficients	$q_{m\ (mg/g)}$	$B_{\ (L/mg)}$	R^2	$K_{f\ (mg/g)}$	n	R^2
Mercury	7.14	0.182	0.9901	1.602	1.917	0.9501

Adsorption kinetics

Adsorption kinetics studies provide an understanding of adsorption rate and controlling mechanism of the process. Kinetic models have been exploited to test the experimental data and to find the mechanism of adsorption and its potential rate-controlling step that includes mass transport and chemical reaction. In addition, information on the kinetics of metal uptake is required to select the optimum conditions for full scale batch or continuous metal removal processes. Adsorption kinetics is expressed as the solute removal rate that controls the residence time of the sorbate in the solid–solution interface. Several kinetic models are available in order to investigate the adsorption mechanisms. These models include Pseudo-first-order rate model and Pseudo-second-order rate model (Rangaraj, 2003), First-order reversible reaction model (Ghosh and Goswami, 2005), Elovich's model (Ho and Mckey, 1998) and intraparticle diffusion model (Rangaraj, 2003). The pseudo-first-order and pseudo-second-order kinetic models were selected to test the adsorption dynamics in this study due to their good applicability in most cases in comparison with the first- and second-order models. The pseudo-first-order rate model based on adsorption capacity of adsorbent is generally expressed as:

$$\ln(q_e-q)=\ln q_e-k_1t$$

where, q_e and q(mg/g) indicate the adsorption capacities at equilibrium and at time t (min), respectively; and k_1 (min^{-1}) is the pseudo-first-order rate constant. Plot of $\ln(q_e-q)$ versus t gives a straight line for first order adsorption kinetics which allows computation of the rate constant k_1. Pseudo-second order model is derived on the basis of adsorption capacity of the solid phase, expressed as:

$$\frac{t}{q}=\frac{t}{q_e}+\frac{l}{k_1q_e^2}$$

The pseudo-second-order rate constant k_1 is determined from experimental data by plotting t/q vs. t. As seen in Figure 11, by plotting qt values versus t, the theoretical q_e, k_1 and k_2 rate constants, and R^2 values were calculated. As can be seen from Table 3, the high R^2 values in the range 0.95 to 0.98 and the good conformity of the theoretical values with experimental values exposed that the adsorption kinetic mechanism of arsenic and mercury onto goethite sorbent can be explained satisfactorily by pseudo-second-order model.

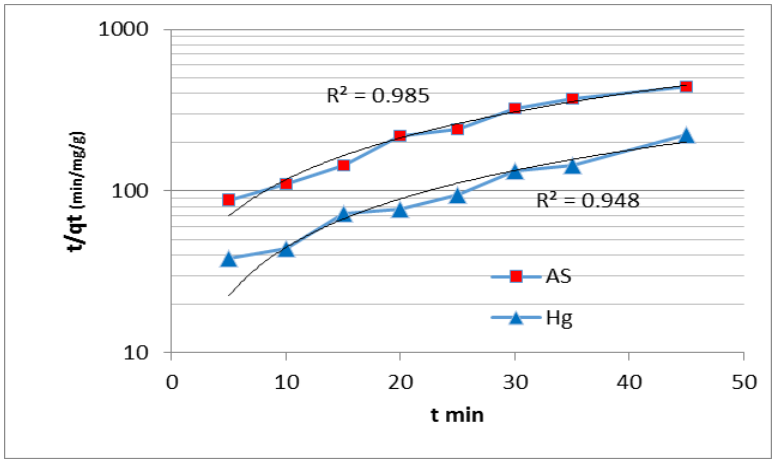

Figure 11. Pseudo-second-order kinetic plots obtained for As and Hg sorption by goethite nanoparticles sorbent.

Table 3. The kinetic constants and correlation coefficients of all kinetic models.

	Pseudo-first-order			Pseudo-second-order		
	K_1 (min^{-1})	q_e(mg/g)	R^2	K_2 (g/mg min)	q_e(mg/g)	R^2
As	0.017	64.15	0.833	0.039	69.2	0.985
Hg	0.195	41.03	0.887	0.210	55.1	0.948

Conclusion

This research showed that the adsorbent dosage, initial arsenic and mercury concentrations, solution pH, temperature, and contact time influenced on the adsorption capacity of the prepared adsorbent significantly. In the removal process of arsenic in mercury by nanoparticles, removal of arsenic at pH=4, adsorbent dose of 4 g/L, time of 120 min and concentration of 10 ppm was about 99.9%, while mercury removal at pH=8, adsorbent dose of 3 g/L, time of 30 min and concentration of 10 ppm was around 72.4%. Furthermore, adsorption studies indicate that both arsenic and mercury have a better trend in Langmuir isotherm than in Freundlich isotherm model. After kinetic evaluation, it became obvious that the pseudo-second-order kinetic reaction model represented the data better for both toxic ions removal processes**.** The results of the present study showed that the synthesized goethite nanoparticles could be appraised as potential adsorbent to remove arsenic and mercury ions from aqueous solutions.

Refrences

Bansal, R., Vastola, F., and Walker, P. 1970. Studies on ultra-clean carbon surfaces-IV. Decomposition of carbon-oxygen surface complexes. Carbon. 8 (4), 443-448.

Bansal, R., Vastola, F., and Walker, P. 1971. Studies on ultra-clean carbon surfaces-III. Kinetics of chemisorption of hydrogen on graphon. Carbon. 9 (2), 185-192.

Bansal, R.C., and Goyal, M. 2005. Activated carbon adsorption. CRC press, 520p.

Beck, J., Vartuli, J., Roth, W.J., Leonowicz, M., Kresge, C., Schmitt, K., Chu, C., Olson, D.H., Sheppard, E., and McCullen, S. 1992. A new family of mesoporous molecular sieves prepared with liquid crystal templates. Journal of the American Chemical Society. 114 (27), 10834-10843.

Blesa, M.A., Magaz, G., Salfity, J.A., and Weisz, A.D. 1997. Structure and reactivity of colloidal metal oxide particles immersed in water. Solid State Ionics. 101, 1235-1241.

Bolong, N., Ismail, A., Salim, M.R., and Matsuura, T. 2009. A review of the effects of emerging contaminants in wastewater and options for their removal. Desalination. 239 (1-3), 229-246.

Cambier, P. 1986. Infrared study of goethites of varying crystallinity and particle size: II. Crystallographic and morphological changes in series of synthetic goethites. Clay Minerals. 21 (2), 201-210.

Chen, H., Wei, G., Han, X., Li, S., Wang, P., Chubik, M., Gromov, A., Wang, Z., and Han, W. 2011. Large-scale synthesis of hierarchical alpha-FeOOH flowers by ultrasonic-assisted hydrothermal route. Journal of Materials Science: Materials in Electronics. 22 (3), 252-259.

Cornell, R.M., and Schwertmann, U. 2003. The iron oxides: structure, properties, reactions, occurrences and uses. John Wiley & Sons, 664p.

Cwiertny, D.M., Hunter, G.J., Pettibone, J.M., Scherer, M.M., and Grassian, V.H. 2008. Surface chemistry and dissolution of α-FeOOH nanorods and microrods: Environmental implications of size-dependent interactions with oxalate. The Journal of Physical Chemistry C. 113 (6), 2175-2186.

Grieger, K.D., Fjordbøge, A., Hartmann, N.B., Eriksson, E., Bjerg, P.L., and Baun, A. 2010. Environmental benefits and risks of zero-valent iron nanoparticles (nZVI) for in situ remediation: risk mitigation or trade-off? Journal of Contaminant Hydrology. 118(3), 165-183.

Jacobson, A.T., and Fan, M. 2019. Evaluation of natural goethite on the removal of arsenate and selenite from water. Journal of Environmental Sciences. 76, 133-141.

Kosmulski, M. 2001. Chemical properties of material surfaces, vol 102. CRC press, 754p.

Langmuir, I. 1918. The adsorption of gases on plane surfaces of glass, mica and platinum. Journal of the American Chemical society. 40 (9), 1361-1403.

Liu, H., Sun, X., Yin, C., and Hu, C. 2008. Removal of phosphate by mesoporous ZrO2. Journal of hazardous materials. 151 (2-3), 616-622.

Lohani, M.B., Singh, A., Rupainwar, D., and Dhar, D. 2008. Studies on efficiency of guava (Psidium guajava) bark as bioadsorbent for removal of Hg (II) from aqueous solutions. Journal of hazardous materials. 159 (2), 626-629.

Lopez-Ramon, M.V., Stoeckli, F., Moreno-Castilla, C., and Carrasco-Marin, F. 1999. On the characterization of acidic and basic surface sites on carbons by various techniques. Carbon. 37 (8), 1215-1221.

Milačič, R., Zuliani, T., Vidmar, J., Bergant, M., Kalogianni, E., Smeti, E., Skoulikidis, N., and Ščančar, J. 2019. Potentially toxic elements in water, sediments and fish of the Evrotas River under variable water discharges. Science of the Total Environment. 648, 1087-1096.

Musić, S., Krehula, S., and Popović, S. 2004. Effect of HCl additions on forced hydrolysis of $FeCl_3$ solutions. Materials letters. 58 (21), 2640-2645.

O'Carroll, D., Sleep, B., Krol, M., Boparai, H., and Kocur, C. 2013. Nanoscale zero valent iron and bimetallic particles for contaminated site remediation. Advances in Water Resources. 51, 104-122.

Rashidi, F., Sarabi, R.S., Ghasemi, Z., and Seif, A. 2010. Kinetic, equilibrium and thermodynamic studies for the removal of lead (II) and copper (II) ions from aqueous solutions by nanocrystalline. Superlattices and microstructures. 48 (6), 577-591.

Sari, A., and Tuzen, M. 2009. Removal of mercury (II) from aqueous solution using moss (Drepanocladus revolvens) biomass: equilibrium, thermodynamic and kinetic studies. Journal of hazardous materials. 171 (1), 500-507.

Saxena, S., Prasad, M., Amritphale, S., and Chandra, N. 2001. Adsorption of cyanide from aqueous solutions at pyrophyllite surface. Separation and Purification Technology. 24 (1), 263-270.

Schwertmann, U., and Cornell, R.M. 2008. Iron oxides in the laboratory: preparation and characterization. John Wiley & Sons.

Su, M., Fang, Y., Li, B., Yin, W., Gu, J., Liang, H., Li, P., and Wu, J. 2019. Enhanced hexavalent chromium removal by activated carbon modified with micro-sized goethite using a facile impregnation method. Science of the total environment. 647, 47-56.

Tripathy, S.S., and Raichur, A.M. 2008. Enhanced adsorption capacity of activated alumina by impregnation with alum for removal of As (V) from water. Chemical Engineering Journal. 138 (1), 179-186.

Vollprecht, D., Krois, L.M., Sedlazeck, K.P., Müller, P., Mischitz, R., Olbrich, T., and Pomberger, R. 2019. Removal of critical metals from waste water by zero-valent iron. Journal of Cleaner Production. 208, 1409-1420.

Wang, L., Fields, K.A., and Chen, A.S. 2000. Arsenic removal from drinking water by ion exchange and activated alumina plants. National Risk Management Research Laboratory, Office of Research and Development, US Environmental Protection Agency, 152p.

Yang, W., Kan, A.T., Chen, W., and Tomson, M.B. 2010. pH-dependent effect of zinc on arsenic adsorption to magnetite nanoparticles. Water research. 44 (19), 5693-5701.